# 8

# The Mean-Field Theory in the Study of Ferromagnets and the Magnetocaloric Effect

J. S. Amaral, S. Das and V. S. Amaral
*Departamento de Física and CICECO, Universidade de Aveiro*
*Portugal*

## 1. Introduction

### List of Symbols

| | | | |
|---|---|---|---|
| $H$ | applied magnetic field | $\beta$ | dependence of $T_C$ in volume |
| $\lambda$ | mean-field exchange parameter | $K$ | compressibility |
| $M$ | magnetization | $\alpha_1$ | thermal expansion |
| $\sigma$ | reduced magnetization | $T_0$ | ordering temperature (no volume coupling) |
| $T$ | temperature | $v$ | volume |
| $\chi$ | magnetic susceptibility | $v_0$ | volume (no magnetic interaction) |
| $N$ | number of spins | $G$ | Gibbs free energy |
| $J$ | spin | $M_{sat}$ | saturation magnetization |
| $g$ | gyromagnetic ratio | $S$ | entropy |
| $\mu_B$ | Bohr magneton | $p$ | pressure |
| $k_B$ | Boltzmann constant | $\eta$ | Bean-Rodbell model parameter |
| $T_C$ | Curie temperature | $\mathcal{B}_J$ | Brillouin function (spin $J$) |
| $\mu_{eff}$ | effective moment | $H_c$ | critical field |
| $C$ | Curie constant | $x$ | fraction of ferromagnetic phase |

Effective field theories, such as the molecular mean-field model (Coey, 2009; Kittel, 1996), are invaluable tools in the study of magnetic materials (Gonzalo, 2006). The framework of the molecular mean-field allows a description of the most relevant thermodynamic properties of a magnetic system, in a simplified way. For this reason, this century-old description of cooperative magnetic effects is still used in ongoing research for a wide range of magnetic materials, although its limitations are well known, such as neglecting fluctuation correlations near the critical temperature and low temperature quantum excitations (Aharoni, 2000).
In this work, we present methodologies and results of a mean-field analysis of the magnetocaloric effect (MCE) (Tishin & Spichin, 2003). The MCE is common to all magnetic materials, first discovered in 1881 by the German physicist Emil Warburg. The effect describes the temperature variation of a ferromagnetic material when subjected to an applied magnetic field change, in adiabatic conditions. In isothermal conditions, there occurs a change in magnetic entropy due to the magnetic field change, and heat is transferred. The first major application of the MCE was presented in the late 1920s when cooling via adiabatic demagnetization was independently proposed by Debye and Giauque. The application of the adiabatic demagnetization process made it possible to reach the very low temperature value of 0.25 K in the early 1930s, by using an applied field of 0.8 T and 61 g of the paramagnetic salt $Gd_2(SO_4)_3 \cdot 8H_2O$ as the magnetic refrigerant.

Pioneered by the ground-breaking work of G. V. Brown in the 1970's, the concept of room-temperature magnetic cooling has recently gathered strong interest by both the scientific and technological communities (Brück, 2005; de Oliveira & von Ranke, 2010; Gschneidner Jr. & Pecharsky, 2008; Gschneidner Jr. et al., 2005; Tishin & Spichin, 2003). The discovery of the giant MCE (Pecharsky & Gschneidner, 1997) resulted in this renewed interest in magnetic refrigeration, which, together with recent developments in rare-earth permanent magnets, opened the way to a new, efficient and environmentally-friendly refrigeration technology.

The development and optimization of magnetic refrigerator devices depends on a solid thermodynamic description of the magnetic material, and its properties throughout the steps of the cooling cycles. This work will present, in detail, the use of the molecular mean-field theory in the study of ferro-paramagnetic phase transitions, and the MCE. The dependence of magnetization on external field and temperature can be described, in a wide validity range. This description is also valid for both second and first-order phase transitions, which will become particularly useful in describing the magnetic and magnetocaloric properties of the so-called "giant" and "colossal" magnetocaloric materials.

An overview of the Weiss molecular mean-field model, and the inclusion of magneto-volume effects (Bean & Rodbell, 1962) is presented, providing the theoretical background for simulating the magnetic and magnetocaloric properties of second and first-order ferromagnetic phase transition systems. The numerical methods employed to solve the transcendental equation to determine the $M(H,T)$ (where $M$ is magnetization, $H$ applied magnetic field and $T$ Temperature) dependence of a ferromagnetic material with a second-order phase transition are described. In the case of first-order phase transitions, the use of the Maxwell construction is shown in order to estimate the equilibrium solution from the two distinct metastable solutions and the single unstable solution of the state equation.

The generalized formulation of the molecular mean-field interaction leads to a novel mean-field scaling method (Amaral et al., 2007), that allows a direct estimation of the mean-field exchange parameters from experimental data. The application of this scaling method is explicitly shown in the case of simulated data, to exemplify its application and to highlight its robustness and general approach. Experimental magnetization data of second (La-Sr-Mn-O based) and first-order (La-Ca-Mn-O based) ferromagnetic manganites is then analyzed under this framework. We show how the Bean-Rodbell mean-field model can adequately simulate the magnetic properties of these complex magnetic systems, candidates for application for room-temperature magnetic refrigerant materials (Amaral et al., 2005; Gschneidner & Pecharsky, 2000; Phan & Yu, 2007).

An overview of the MCE is presented, focusing on the use of the Maxwell relations to estimate the magnetic entropy change of a magnetic phase transition. The thermodynamics of the molecular mean-field model presents us also a new method to estimate the MCE from magnetization data. Results of magnetic entropy variation values are compared, highlighting the difficulties of estimating the MCE in first-order phase transition systems.

The interest on the magnetocaloric properties of first-order phase transition systems, in terms of fundamental physics and also magnetic refrigeration applications, has opened debate on the validity of the use of Maxwell relations to estimate the MCE in these systems (Giguère et al., 1999). Using simulated data of a first-order mean-field system, we verify the consequences of the common use of the Maxwell relation to estimate the MCE from non-equilibrium magnetization data.

The recent reports of "colossal" values of magnetic entropy change of first-order phase transition systems (de Campos et al., 2006; Gama et al., 2004; Rocco et al., 2007) are also discussed, and are shown to be related to the mixed-phase characteristics of the system. We present a detailed description on how the misuse of the Maxwell relation to estimate the MCE of these systems justifies the non-physical results present in the bibliography (Amaral & Amaral, 2009; 2010).
Understanding the thermodynamics of a mixed-phase ferromagnetic system allows the construction of a new methodology to correct the results from the use of the Maxwell effect on magnetization data of these compounds. This methodology is theoretically justified, and its application to mean-field data is presented (Das et al., 2010a;b). In contrast to other suggestions in the bibliography (Tocado et al., 2009), this novel methodology permits a realistic estimative of the magnetic entropy change of a mixed-phase first-order phase transition system, with no need of additional magnetic or calorimetric measurements.

## 2. Molecular mean-field theory and the Bean-Rodbell model

### 2.1 Ferromagnetic order and the Weiss molecular field

A simplified approach to describing ferromagnetic order in a given magnetic material was put forth by Weiss, in 1907. This concept of a molecular field assumes the magnetic interaction between magnetic moments as equivalent to the existence of an additional internal interaction/exchange field that is a function of the bulk magnetization $M$:

$$H_{total} = H_{external} + H_{exchange} \text{ and } H_{exchange} = \lambda M, \tag{1}$$

where $\lambda$ is the mean-field exchange parameter.
The general representation of the molecular mean-field model is then

$$\sigma = f\left[\frac{H + \lambda M}{T}\right]. \tag{2}$$

where $f$ is the general function that applies in the paramagnetic system (e. g. the Brillouin function).
From a linear approximation of the susceptibility (Curie law):

$$\chi = \frac{M}{H} = \frac{NJ(J+1)g^2\mu_B^2}{3k_BT_C} = \frac{N\mu_{eff}^2}{3k_BT_C}; \tag{3}$$

where $\mu_{eff}$ is the effective magnetic moment: $\mu_{eff} = g[J(J+1)]^{1/2}\mu_B$.
We define the Curie temperature $T_C$ as the temperature where the ferromagnetic to paramagnetic transition occurs, and there is a divergence in the susceptibility:

$$\chi = \frac{C}{T - T_C}, \text{ where } C = \frac{NJ(J+1)g^2\mu_B^2}{3k_B} \text{ and } T_C = C\lambda. \tag{4}$$

The exchange parameter can be estimated from the following relation, as long as $N$ and $J$ are known.

$$\lambda = \frac{3k_BT_C}{Ng^2J(J+1)\mu_B^2} \tag{5}$$

Typical values of $\lambda$ correspond to molecular fields in the order of hundreds of Tesla.

### 2.2 Magneto-volume effects: The Bean-Rodbell model

The Bean-Rodbell model (Bean & Rodbell, 1962) adds a phenomenological description of magneto-volume effects to the classical molecular mean-field model of Weiss. The dependence of exchange interaction on interatomic spacing is then considered, taking into account three new parameters: $\beta$, which corresponds to the dependence of ordering temperature on volume, and also the volume compressibility, $K$ and thermal expansion $\alpha_1$. The formulation behind the model is as follows:

$$T_C = T_0 \left[ 1 + \beta \left( \frac{v - v_0}{v_0} \right) \right] , \tag{6}$$

where $T_C$ is the Curie temperature corresponding to a lattice volume of $v$, while $v_0$ is the equilibrium lattice volume in the absence of magnetic interactions, corresponding to a Curie temperature of $T_0$ if magnetic interactions are assumed, but with no magneto-volume effects. The free energy of the system can therefore be described, taking into account magnetic and volume interactions. For simplicity, we consider a purely ferromagnetic interaction. For a description including anti-ferromagnetic interactions, see Ref. (Bean & Rodbell, 1962).

$$G = G_{\text{field}} + G_{\text{exchange}} + G_{\text{volume}} + G_{\text{pressure}} + G_{\text{entropy}} \tag{7}$$

Considering first a spin 1/2 system, and the molecular field exchange interaction, we have that the Gibbs free energy per unit volume is:

$$\begin{aligned} G_v = & -HM_{sat}\sigma - \frac{1}{2}Nk_BT_c\sigma^2 + \frac{1}{2K}\left[\frac{v - v_0}{v_0}\right]^2 + p\left(\frac{v - v_0}{v_0}\right) \\ & - TNk_B\left[\ln 2 - \frac{1}{2}\ln\left(1 - \sigma^2\right) - \sigma \tanh^{-1}\sigma\right] - TS_{\text{lattice}}. \end{aligned} \tag{8}$$

where $\sigma$ is the reduced magnetization, $M_{sat}$ the saturation magnetization and $N$ the number of particles for volume $v_0$. While the original description of Bean and Rodbell does not initially consider the lattice entropy, we will keep the generality of the calculations along our description of the model. The lattice entropy term is as follows:

$$S_{\text{lattice}} = 3Nk_B\left[\frac{x}{e^x - 1} - ln(1 - e^{-x})\right], \tag{9}$$

where $x \equiv h\nu/k_BT$ with $\nu$ being the phonon frequency. Eq. 9 can be expanded via the Debye approximation:

$$S_{\text{lattice}} = Nk_B\left[4 - 3\ln\Theta/T + (3/40)(\Theta/T^2) + ...\right] \tag{10}$$

where $\Theta \equiv h\nu_{\max}/T$. From the previous expression we obtain:

$$\partial S/\partial v \cong -3Nk_Bd\ln(\nu_{\max})/dv = \alpha_1/K \tag{11}$$

where $\alpha_1$ is the thermal expansion coefficient ($\alpha_1 \equiv (1/v)(\partial v/\partial T)_p$) and $K$ is the compressibility ($K \equiv -(1/v)(\partial v/\partial p)_T$).

By substituting Eq. 6 into Eq. 8, deriving in volume by using also Eq. 11, the relation between magnetization and volume that corresponds to the energy minimum is

$$\frac{v - v_0}{v_0} = \frac{1}{2} N K k_B T_0 \beta \sigma^2 + T v_o \alpha_1 - pK \tag{12}$$

By substituting the previous relation into the Gibbs free energy (Eq. 8), and minimizing in respect to volume, we obtain

$$\begin{aligned} (G_v)_{\min} = & -HM_{sat}\sigma - \frac{1}{2} N k_B T_0 \sigma^2 \left[1 - \beta(pK - \alpha_1 T)\right] \\ & - p^2 K/2 - \alpha_1^2 T^2/2K + \alpha_1 T p - \frac{1}{2K}(\frac{1}{2} N k_B T_0 \sigma^2 \beta)^2 \\ & - TNk_B \left[4 + \ln 2 - \frac{1}{2}\ln(1 - \sigma^2) - \sigma \tanh^{-1}\sigma\right]. \end{aligned} \tag{13}$$

By minimizing as a function of $\sigma$, we obtain the implicit dependence of $\sigma$ on temperature, for spin 1/2.

$$\frac{T}{T_0} = \frac{\sigma}{\tanh^{-1}\sigma}\left(1 - \beta(pK - \alpha_1 T) + \frac{\eta\sigma^2}{3} + M_{sat}H\right) \tag{14}$$

where the $\eta$ parameter defines the order of the phase transition, if $\eta \leq 1$, the transition is second-order and if $\eta > 1$, the transition is first-order. The value of $\eta$ is:

$$\eta = \frac{3}{2} N k_B K T_0 \beta^2 \ \text{; (spin = 1/2)} \tag{15}$$

$$\eta_J = \frac{5}{2}\frac{[4J(J+1)]^2}{\left[(2J+1)^4 - 1\right]} N k_B K T_0 \beta^2 \ \text{; (arbitrary J spin).} \tag{16}$$

We can rewrite Eq. 14, in the more familiar molecular-mean field expression type, $M = f[(H + \lambda \mathrm{M})/\mathrm{T}]$, since $\tanh^{-1}\sigma = (H + \lambda(M,T)M)/T$, (for spin = 1/2):

$$\tanh^{-1}\sigma = \frac{g\mu_B H/2k_B + (1 - \beta pK + \beta\alpha_1 T)T_0\sigma + (\eta/3)T_0\sigma^3}{T}. \tag{17}$$

We can therefore consider, in the absence of external pressure, and considering the lattice entropy change small, that the molecular field dependence in magnetization follows the simple form of $H_{\text{exchange}} = \lambda_1 M + \lambda_3 M^3$.

Considering a generalized spin system, with no applied pressure, nor the lattice entropy contribution, the implicit dependence of $\sigma$ on temperature is

$$T(\sigma, H) = \frac{g\mu_B JH/k_B + aT_0\sigma + bT_0\sigma^3}{\mathcal{B}_J^{-1}(\sigma)}, \tag{18}$$

where

$$a = \frac{3J}{J+1}; \qquad b = \frac{9}{5}\frac{(2J+1)^4 - 1}{(2(J+1))^4}\eta_J = b'\eta_J \tag{19}$$

and ${\mathcal{B}_J}^{-1}(\sigma) = \partial S_J/\partial\sigma$, where $\mathcal{B}_J$ is the Brillouin function for a given $J$ spin.

If the lattice entropy change is taken into consideration, the effect corresponds introducing the $\beta\alpha_1 T$ term into the first-order term of the exchange field, in the same way as the spin 1/2 system.
If we choose to describe the exchange field as $\lambda_1 M + \lambda_3 M^3$, it becomes practical to rewrite the conditions of the model explicitly in terms of the $\lambda_1$ and $\lambda_3$ parameters, bulk magnetization $M$, spin and the saturation magnetization, $M_{sat}$. This corresponds to the following expression, where the $\eta$ parameter can be defined as:

$$\eta = \lambda_3 / \left[ b' T_0 k_B / (g \mu_B J^2 M_{\mathrm{sat}}^3) \right], \tag{20}$$

where the $b'$ parameter is previously defined in Eq. 19. The $\lambda_3$ parameter includes the $\beta$ (dependence of ordering temperature on volume) and $K$ (compressibility) system variables. The direct consequence of the previous expression is that, by substituting the $T_0$ value, the ratio of $\lambda_1$ and $\lambda_3$, together with the system parameters define the nature of the transition, following the next simplified expression:

$$\eta = \frac{3J^2 M_{sat}^2}{b'} \frac{\lambda_3}{\lambda_1}. \tag{21}$$

### 2.3 Numerical approach

#### 2.3.1 Second-order phase transitions

As shown in the previous section, the Bean-Rodbell model can describe a magnetovolume induced first-order phase transition. While the numerical approach to simulate first-order phase transitions in the Landau theory is straightforward (finding the roots of a polynomial and then which of the two local minima corresponds to the absolute free energy minimum), in the case of the Bean-Rodbell model the case is more complicated in computational terms. Even in the more simple second-order phase transition, solving the transcendental equation $M = f[(H + \lambda M)/T]$ cannot be done algebraically, and so numerical methods are employed. The classic visual representation of the numerical approach is presented in Fig. 1.

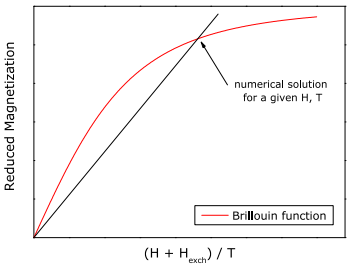


Fig. 1. Graphical solution of the mean-field state equation, adapted from Ref. (Kittel, 1996).

This graphical approach is easily converted into numerically finding the roots of the following function:

$$M_{\mathrm{sat}} \mathcal{B}_J(J, \lambda_1, \lambda_3, M, H, T) - M(H, T); \tag{22}$$

Finding the roots of the above equation can be numerically achieved by using the optimized method suggested by T. Dekker, employing a combination of bisection, secant, and inverse quadratic interpolation methods (Forsythe et al., 1976).

### 2.3.2 First-order phase transitions

For the first-order phase transition, there are multiple solutions that need to be calculated, corresponding to the stable (equilibrium), metastable and unstable branches. Fig. 2(a) shows a representation of these solutions.

The methodology for obtaining the various $M$ solutions in this situation is more numerically intensive than in a second-order system, apart from subdividing the interval of magnetization values into multiple sub-intervals to search for the multiple roots.

In order to calculate the critical field value $H_c$ and consequently the full equilibrium solution (stable branch), the Maxwell construction (Callen, 1985) is applied, which consists of matching the energy of the two phases, in the so-called equal-area construction (Fig. 2(b)).

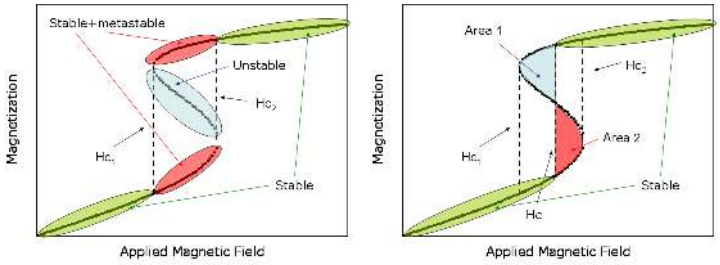


(a) (b)

Fig. 2. a) The multiple solution branches from the roots of Eq. 22, for a first-order transition from the Bean-Rodbell model, and b) the Maxwell construction for determining the critical field $H_c$ and the full equilibrium solution, for a first-order magnetic phase transition system.

In numerical terms, applying this graphical methodology becomes a matter of integrating the areas between the metastable and unstable solutions, between the $Hc_1$ and $Hc_2$ field values, until the value of area 1 is equal to area 2. This operation is numerically intensive, but manageable for realistic field interval values. The most important numerical concern is adequately reproducing all branches (solutions), in a way that the algorithm correctly integrates each area. In programming terms, this becomes a complicated problem, but becomes controllable by a careful definition of the various number of roots of the functions, and developing an optimized integration algorithm for each independent situation that can appear within this approach.

### 2.3.3 Estimating magnetic entropy change

Within the molecular field model, the relation between the magnetic entropy and the magnetic equation of state is simply defined. Let us consider that the magnetic equation of state is a generalized $f$ function, and so $M = f[(H + \lambda(M,T)M)/T]$. We can then integrate the magnetic entropy relation:

$$S_M = \int f^{-1}(M)dM. \tag{23}$$

So to calculate the entropy change between two distinct field values $H_1$ and $H_2$:

$$-\Delta S_M(T)_{\Delta H} = \int_{M|_{H_1}}^{M|_{H_2}} f^{-1}(M)dM. \tag{24}$$

where $f^{-1}(M)$ is simply the argument of the state function for a given magnetization value:

$$f^{-1}(M) = \frac{H + \lambda(M,T)M}{T}. \tag{25}$$

We can generalize the previous result by considering an explicit dependence of the exchange field in temperature. We rewrite the previous equation as

$$f^{-1}(M) = \frac{H}{T} + \frac{\lambda(M,T)M}{T} \rightarrow H = Tf^{-1}(M) - \lambda(M,T)M \tag{26}$$

and using the following Maxwell relation (Callen, 1985):

$$\left(\frac{\partial S}{\partial M}\right)_T = -\left(\frac{\partial H}{\partial T}\right)_M, \tag{27}$$

entropy can be estimated by

$$\Delta S(T)_{H_1 \rightarrow H_2} = -\int_{M_{H1}}^{M_{H2}} \left(\frac{\partial H}{\partial T}\right)_M dM, \tag{28}$$

leading to

$$-\Delta S_M(T)_{H_1 \rightarrow H_2} = \int_{M|_{H_1}}^{M|_{H_2}} \left(f^{-1}(M) - \left(\frac{\partial \lambda}{\partial T}\right)_M M\right) dM. \tag{29}$$

Compared to Eq. 24, the derivative $\partial\lambda/\partial T$ directly affects the result. We shall explore the use of Eq. 24 to calculate the magnetic entropy change and compare it to the use of the Maxwell relation.

## 3. A molecular mean-field scaling method

### 3.1 Methodology

As presented in section 2.2, the molecular mean-field theory gives us a simple and often effective tool to describe a ferromagnetic system. If one is studying magnetization data from a given material, obtaining the mean-field parameters is not immediate. To do so, one usually needs to set the spin value and/or the number of ions $N$, and the mean-field state function is the Brillouin function or Langevin function (for a high spin value). From then on, the $\lambda_1$ parameter can be obtained from low-field $M$ versus $T$ measurements and a linear Curie-Weiss law fit of the inverse susceptibility. Subsequent fits to each $M(H)$ isotherm can then be performed. Such an approach can be quite complex, particularly if one considers a system where the magnetic ions can have different spin states, such as mixed-valence manganites, where the ratio between ions needs to be previously assumed (Szewczyk et al., 2000). Obtaining higher orders of the mean-field exchange parameter ($\lambda_3$, $\lambda_5$, etc.) can be done by performing simulations to describe experimental data, as done by Bean and Rodbell to describe MnAs (Bean & Rodbell, 1962).

A different approach to obtain the mean-field parameters from experimental magnetization data is presented here, based on data scaling. A summarized version of this work has been published in 2007 (Amaral et al., 2007). We consider the general mean field law, $M(H,T) = f((H + H_{exch})/T)$, where the state function $f$ is not pre-determined, and that $\lambda$ (as in $H_{exch} = \lambda M$) may depend on $M$ and/or $T$. Then for corresponding values with the same $M$, $(H + H_{exch})/T)$ is also the same, the value of the inverse $f^{-1}(M)$ function:

$$\frac{H}{T} = f^{-1}(M) - \frac{H_{exch}}{T} \tag{30}$$

By taking $H$ and $T$ groups of values for a constant $M$ and Eq. 30, the plot of $H/T$ versus $1/T$ is linear if $\lambda$ does not depend on $T$. The slope is then equal to $H_{exch}$, for each $M$ value. Then, each isomagnetic line is shifted from the others, since its abscissa at $H/T = 0$ is simply the inverse temperature of the isotherm which has a the spontaneous magnetization equal to the $M$ value (Fig. 3).

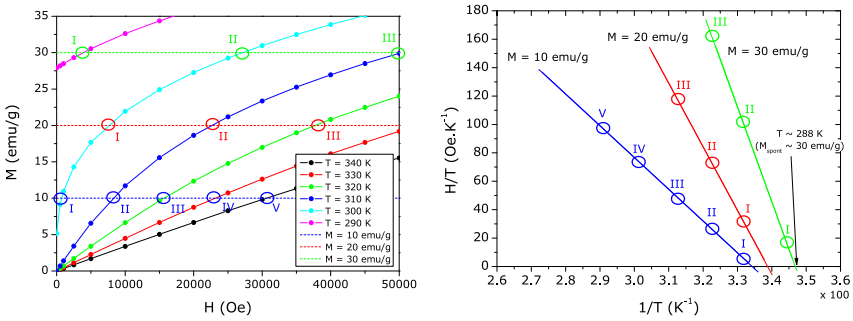


(a) (b)

Fig. 3. a) Isomagnetic ($M = 10$, 20 and 30 emu/g) points from mean-field generated data in an $M$ versus $H$ plot (lines are eye-guides), and b) corresponding $H/T$ versus $1/T$ plot (lines are linear fits to isomagnetic points).

In a similar fashion, a simple case of a constant $\lambda$ (i. e. independent of $M$ and $T$), a plot of $H/MT$ versus $1/T$ will show parallel lines for all $M$ values, with slope equal to $H_{exch}/M$, which in turn is equal to $\lambda$.

In a first-order phase transition, the discontinuity of $M(H,T)$ means that when interpolating data for constructing the isomagnetic curves, care should be taken not to interpolate the discontinuity in $M(H,T)$. This is shown in Fig. 4 and is a direct consequence of there being a region in the $H/T$ versus $1/T$ plot that has no data, much like the preceding $M(H,T)$ plot.

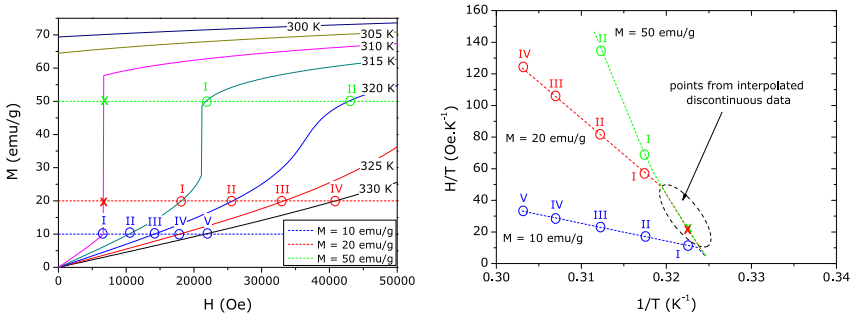


(a) (b)

Fig. 4. a) Isomagnetic ($M = 10$, 20 and 30 emu/g) points from mean-field generated data in an $M$ versus $H$ plot (lines are eye-guides), and b) corresponding $H/T$ versus $1/T$ plot (lines are linear fits to isomagnetic points).

Extrapolating this linear relation within this region will not present any real physical result, namely any relation to the spontaneous magnetization, which has a discontinuous jump. This point will be clearer in further simulation results.
From Eq. 30, the dependence of the exchange field on $M$ is obtained directly. In principle, one can expect that the exchange field is given by a series of odd powers of $M$, $H_{exch} = \lambda M = \lambda_1 M + \lambda_3 M^3 + \ldots$. This follows from the frequently found expansion of the free energy in powers of $M$, e.g. when considering magnetovolume effects within the mean-field model by the Bean-Rodbell model as described in section 2.2. Note that the demagnetizing factor is intrinsically taken into account as a constant contribution to $\lambda_1$:

$$H_{total} = H_{applied} + H_{exch} - DM = H_{applied} + (\lambda_1 - D)M + \lambda_3 M^3 + \ldots \tag{31}$$

where $D$ is the demagnetizing factor, in the simple assumption of an uniform magnetization. After obtaining $H_{exch}$, the second step of this method consists on building the scaling plot of $M$ versus $(H + H_{exch})/T$, where data should collapse to the one curve that describes the system, the $f$ function. Analyzing the $f$ function is a further important step to study magnetic systems and to compare the results of theoretical microscopic models.
The above mentioned collapse on the scaling plot can be used to evaluate the validity of the mean-field analysis. In this sense the method is self-consistent: only if $H_{exch}$ has been properly evaluated, will the points collapse into a single curve.

### 3.1.1 Second-order phase transition

As a first immediate example of this methodology, let us consider mean-field generated data, for a spin 2 system, with saturation magnetization of 100 emu $g^{-1}$ and $T_C \sim 300$ K. No dependence of $\lambda$ on $T$ was considered. $M$ versus $H$ data, from 290 to 330 K, at a 1 K temperature step and 100 Oe feld step, are shown in Fig. 5(a).

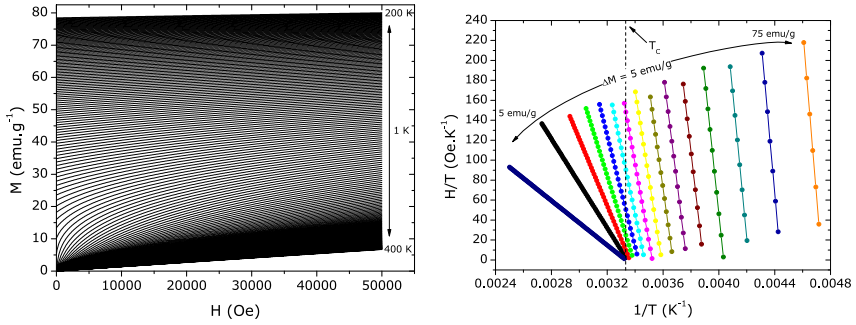


(a) (b)

Fig. 5. a) Isothermal magnetization versus applied magnetic field, from 200 to 400 K, at a 1 K temperature step and 100 Oe field step and b) Isomagnetic $H/T$ versus $1/T$ plot, of data from the molecular mean-field model, from $M = 5$ emu/g (dark blue line) to $M = 75$ emu/g (orange line), with a 5 emu/g step.

We then plot $H/T$ versus $1/T$ at constant values of magnetization, following Eq. 30 (Fig. 5(b)). Since $\lambda$ does not depend on $T$, there is a linear behavior of the isomagnetic curves, which are progressively shifted into higher $1/T$ values. From Eq. 30, the slope of each isomagnetic line of Fig. 5(b) will then give us the dependence of the exchange field in $M$ (Fig. 6(a)).

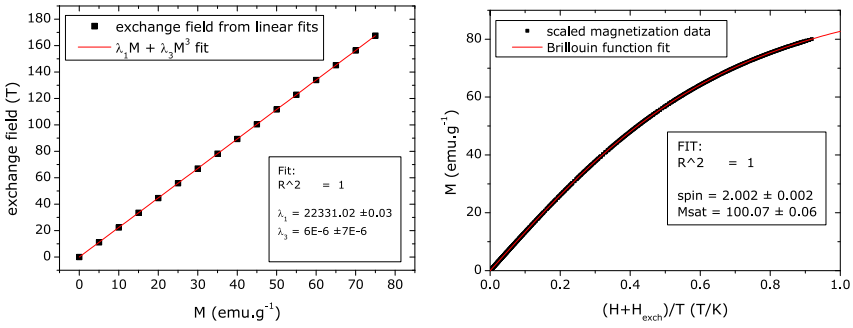


(a) (b)

Fig. 6. a) Fit of the exchange field dependence on $M$. Solid squares represent the slope of each isomagnetic curve, from Figure 5(b) and b) Brillouin function fit of scaled data from the mean-field model, from Figure 5(a).

Having determined the $\lambda(M)$ dependence, we can now proceed to scale all the magnetization data, to determine the mean-field state function (Fig. 6(b)).
As expected, the scaled data closely follows a Brillouin function, with spin 2, and a saturation magnetization of 100 emu $g^{-1}$. We can then describe, interpolate and extrapolate $M(H,T)$ at will, since the full mean-field description is complete (exchange parameters and state function).

### 3.1.2 First-order phase transition

As shown previously, this approach is also valid if a first-order magnetic phase transition in considered. There is no fundamental difference on the methodology, apart from the expected higher order terms of $\lambda(M)$. Care must be taken when interpolating $M(H)$ data within the irreversibility zone, so that no values of $M$ correspond to the discontinuities. We simulate a first-order magnetic phase transition by adding a $\lambda_3$ dependence of the molecular exchange field, equal to 1.5 (Oe $emu^{-1}$ $g)^3$, to the previous second-order transition parameters. Isothermal magnetization data is shown in Fig 7(a). The discontinuity in magnetization values is visible, and we can estimate that the critical field is around 2.5 T, for this simulation parameters.
From the $M(H,T)$ data, we plot the corresponding isomagnetic $H/T$ versus $1/T$ plot (Fig. 7(b)).
As shown previously in Fig. 4 b), if interpolations in $M(H,T)$ are done within the discontinuities, points that do not follow the expected linear behavior appear. These points should not be included for the linear fits to determine $\lambda(M)$. In the rest of the plot, the linear relation between $H/T$ and $1/T$ is kept, as expected. Linear fits are then easily made to each isomagnetic line, and we obtain the exchange field dependence on magnetization (Fig. 8(a)).
The $\lambda_1 M + \lambda_3 M^3$ dependence of the mean-field exchange parameter is well defined. We obtain $\lambda_1$ and $\lambda_3$ values that are, within the fitting error, equivalent to the initial parameters. This shows us that the first-order nature of the transition and the associated discontinuities should not affect this mean-field scaling methodology.
We can then construct the scaling plot, using the obtained $\lambda_1$ and $\lambda_3$ parameters (Fig. 8(b)). From the scaling plot and the subsequent fit with the Brillouin function, we obtain values of spin and saturation magnetization close to the the initial parameters of the simulation.

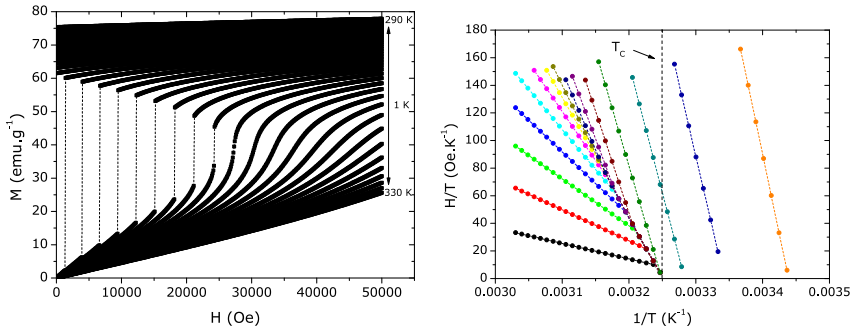


Fig. 7. a) Isothermal $M$ versus $H$ data of a first-order magnetic phase transition, from the Bean-Rodbell model and b) corresponding isomagnetic $H/T$ versus $1/T$ plot, for a first-order mean-field system, and a 5 emu $g^{-1}$ step.

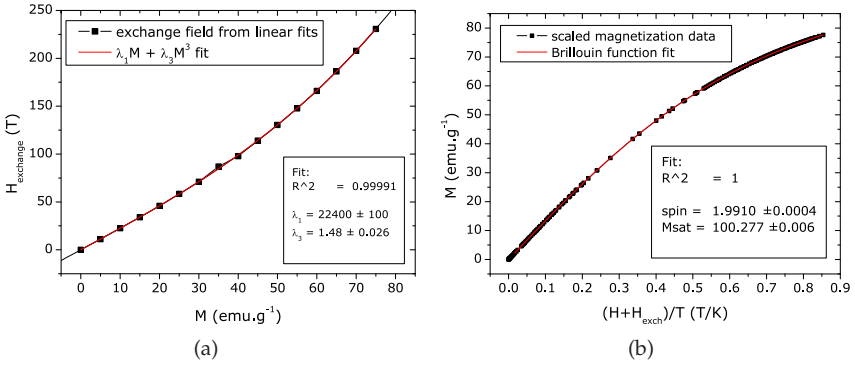


Fig. 8. a) Exchange field fit for a first-order mean-field system, with the $\lambda_1 M + \lambda_3 M^3$ law, and b) corresponding mean-field scaling plot and Brillouin function fit.

### 3.2 Applications

In the previous section, we have shown how it is possible to obtain directly from bulk magnetization data, and only considering the mathematical properties of the general mean-field expression $M = f[(H + \lambda M)/T]$, a direct determination of the molecular field exchange parameter $\lambda$ and its dependence on $M$, and the mean-field state function $f$, which will contain information on the magnetic entities in play, and their interactions.

One immediate application for this method is to use this description of the magnetic properties of the system as a way to interpolate/extrapolate experimental data, and/or as a smoothing criteria to noisy $M(H,T)$ and corresponding $\Delta S_M(T)$ curves. It is worth mentioning that while this can be also performed within Landau theory, since the mean-field theory is not limited to small $M$ values, the mean-field description of the system can have a broader application range: lower $T$ and higher $H$ values, up to saturation. Still, the methodology presented here is time-consuming, even with optimized numerical data analysis programs. When considering experimental magnetization data for $T < T_C$, care must be taken to adequately disregard data from the magnetic domain region (low fields). Still, the ability

to determine the mean-field parameters directly from experimental data becomes attractive taking in mind that one can estimate magnetic entropy (and consequently magnetic entropy change) within the mean-field model, by using Eq. 29, reproduced here for convenience.

$$-\Delta S_M(T)_{H_1 \to H_2} = \int_{M|_{H_1}}^{M|_{H_2}} \left( f^{-1}(M) - \left( \frac{\partial \lambda}{\partial T} \right)_M M \right) dM.$$

And so not only can the $M(H,T)$ values be interpolated/extrapolated, the entropy curves and their dependence in field and temperature can also be easily interpolated and extrapolated as well. This becomes particularly appealing if one wishes to make thermal simulations of a magnetic refrigeration device, and, within a physical model (and not by purely numerical approximations), the magnetocaloric response of the material, at a certain temperature and a certain field change is directly calculated. As an example of this approach, bulk isothermal magnetization data of two ferromagnetic manganite systems will be analyzed in this section. Fig. 9(a) shows the magnetization data of the ferromagnetic, second-order phase transition $La_{0.665}Er_{0.035}Sr_{0.30}MnO_3$ manganite, obtained by SQUID measurements. Fig. 9(b) shows the isomagnetic $H/T$ versus $1/T$ plot, up to 50 emu/g in a 5 emu/g step, which could be reduced in order to have more points.

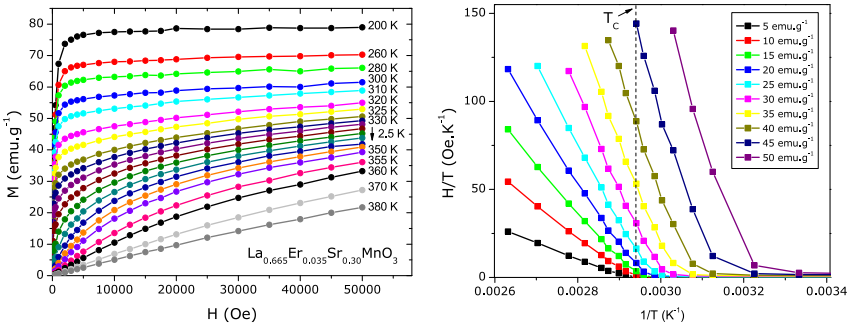


(a) (b)

Fig. 9. a) Magnetization data of $La_{0.665}Er_{0.035}Sr_{0.30}MnO_3$ and b) corresponding isomagnetic $H/T$ versus $1/T$ plot. Lines are eye-guides.

Each point at constant $M$ is obtained from data interpolation os the isothermal $M(H)$ data. From linear fits to the $H/T$ versus $1/T$ plot, the dependence of the exchange field in magnetization is directly obtained (Fig. 10(a)). The exchange field is fitted to a $\lambda_1 M + \lambda_3 M$ function. The scaling plot is then constructed (Fig. 10(b)).

For calculation purposes, the scaling function of Fig. 10(b) was described as an odd-terms polynomial function. The Fig. shows some data point that are clearly deviated from the scaling function. These points correspond to the magnetic domain region (low fields, $T < T_C$). With the exchange field and mean-field state function described, the magnetic behavior of this material can then be simulated. Also, magnetic entropy change can be calculated from the mean-field relation of Eq. 29. Result from these calculations, together with the experimental $M(H,T)$ data and $\Delta S_M(H,T)$ results from Maxwell relation integration are shown in Fig. 11. A good agreement between the experimental $M(H,T)$ curves and the mean-field generated curves with the obtained parameters is obtained. The entropy results show some deviations, particularly near $T_C$. While the mean-field theory does not consider fluctuations near

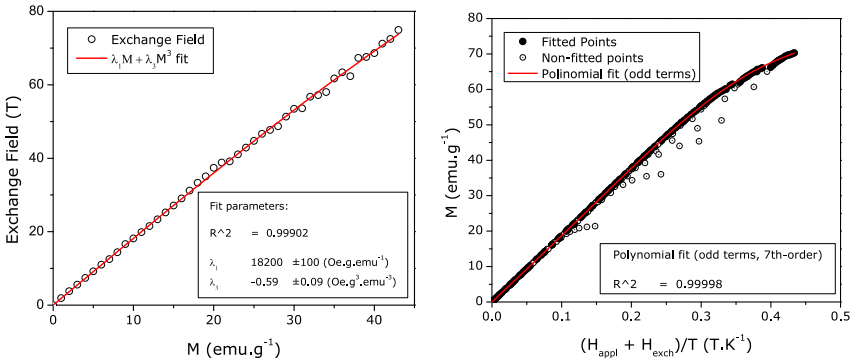


Fig. 10. Interpolating a) experimental $M(H,T)$ data and b) magnetic entropy change results by mean-field simulations for the second-order phase transition manganite $La_{0.665}Er_{0.035}Sr_{0.30}MnO_3$.

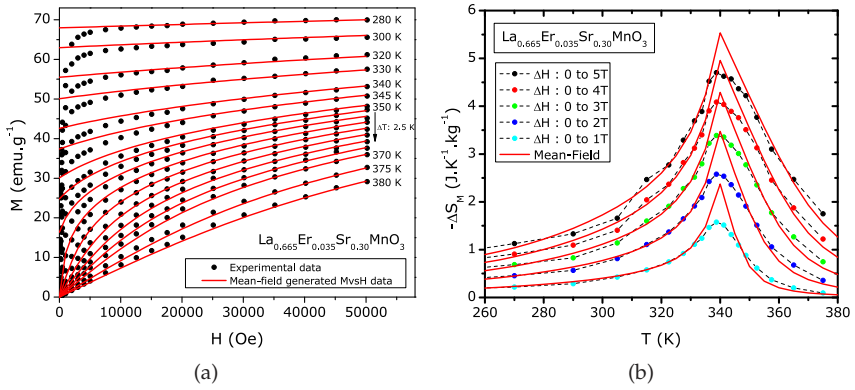


Fig. 11. Interpolating a) experimental $M(H,T)$ data and b) magnetic entropy change results by mean-field simulations for the second-order phase transition manganite $La_{0.665}Er_{0.035}Sr_{0.30}MnO_3$.

$T_C$, these deviations can be attributed to that fact. Still, by considering disorder effects (chemical/structural inhomogeneity), a better description of magnetocaloric properties can be obtained (Amaral et al., 2008).

We now consider bulk magnetization data of a the first-order ferromagnetic phase transition $La_{0.638}Eu_{0.032}Ca_{0.33}MnO_3$ manganite. Fig. 12(a) shows isothermal magnetization data obtained from SQUID measurements, and Fig. 12(b) shows the corresponding isomagnetic $H/T$ versus $1/T$ plot.

The exchange field $H_{exch}$ dependence on magnetization (Fig. 13(a)) and the mean-field state function (Fig. 13(b)) are then obtained.

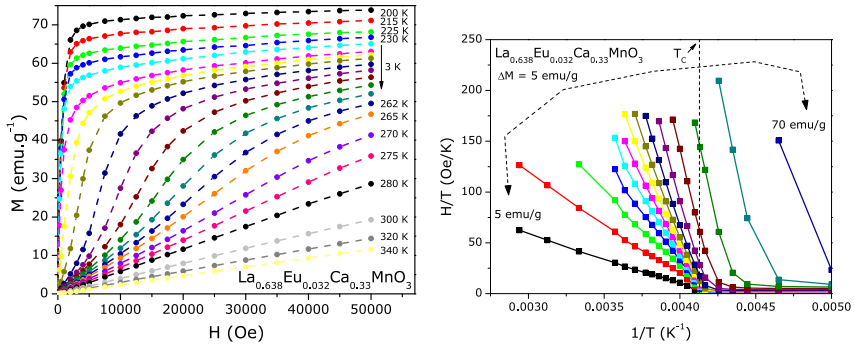


(a) (b)

Fig. 12. a) Magnetization data of $La_{0.638}Eu_{0.032}Ca_{0.33}MnO_3$ and b) corresponding isomagnetic $H/T$ versus $1/T$ plot. Lines are eye-guides.

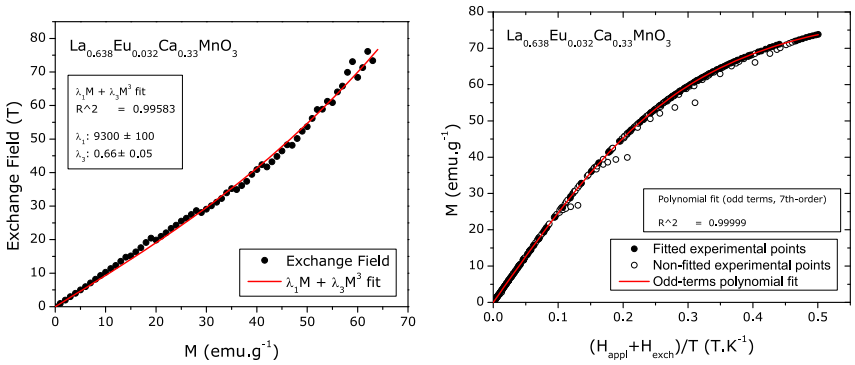


(a) (b)

Fig. 13. Interpolating a) experimental $M(H,T)$ data and b) magnetic entropy change results by mean-field simulations for the second-order phase transition manganite $La_{0.665}Er_{0.035}Sr_{0.30}MnO_3$.

Like the previous example of the second-order manganite, the mean-field state function $f$ is fitted to a polynomial function, for calculation purposes. With the $\lambda_1$ and $\lambda_3$ exchange parameters and the $f$ function described, $M(H,T)$ simulations can be performed, and compared to the experimental values. Also, magnetic entropy change can be estimated from the mean-field relation of Eq. 29 and compared to results form the use of the Maxwell relation. Results are shown in Fig. 14.

The results of this mean-field scaling method are also very promising for this first-order phase transition system. The insight that can be gained from the use of this methodology for a given magnetic system can be of great interest. In a simplistic approach, we can say that if this scaling method does not work, then the system does not follow a molecular mean-field behavior, and other methods need to be pursued in order to interpret the magnetic behavior of the system. It is important to emphasize that this scaling analysis is global, in the sense that it encompasses the consistency of the whole set of magnetization data.

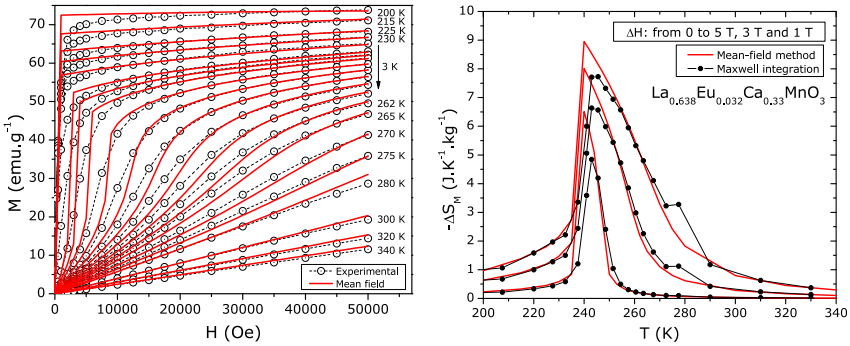


Fig. 14. Interpolating a) experimental $M(H,T)$ data and b) magnetic entropy change results by mean-field simulations, of the first-order phase transition manganite $La_{0.638}Eu_{0.032}Ca_{0.33}MnO_3$.

### 3.3 Limitations

Of course, there are limitations to the use of this method, even if one is successful in determining the exchange field parameters and, from what appears to be a good scaling plot, determine the mean-field exchange function. For extensive and smooth $M(H,T)$ data, interpolating isomagnetic data should not pose a real problem, but choosing which points in the $H/T$ versus $1/T$ to fit or to disregard (due to magnetic domains or from the discontinuities of first-order transitions) can remove the confidence on the final scaling plot, and consequently on the mean-field state function.

This simple approach also does not take into account any potencial explicit dependence of the exchange field on temperature. While this dependence is possible, it is generally not considered in the molecular mean-field framework. On the examples we have shown earlier, no such $\lambda(T)$ dependence was considered.

Nevertheless, the best way to evaluate if the mean-field model and obtained parameters are able to describe experimental data is to compare simulations to experiment.

## 4. The magnetocaloric effect in first-order magnetic phase transitions

### 4.1 Estimating magnetic entropy change from magnetization measurements

The most common way to estimate the magnetic entropy change of a given magnetic material is from isothermal bulk magnetization measurements. To this effect, one has to simply integrate the Maxwell relation. However, the validity of this approach has been questioned for the case of a first-order magnetic phase transition. The first argument comes from purely numeric considerations, since the discontinuities of the thermodynamic parameters, common to first-order transitions, will make the usual numerical approximations less rigorous in their vicinity. Since the first reports of materials presenting the giant MCE, anomalous 'spikes' in the $\Delta S_M(T)$ plots are commonly seen in literature, for first-order systems. This so-called magnetocaloric peak effect, is present in results form magnetization measurements, but does not appear in calculations using specific heat data.

Indeed, the most immediate culprit for these peaks to occur would be the numerical approximations, which become less rigorous near the transition (Wada & Tanabe, 2001). The

peak effect has also been discussed in other perspectives, most notably by Pecharsky and Gschneidner (Pecharsky & Gschneidner, 1999) and Giguère *et al.* (Giguère et al., 1999), for the case of $Gd_5Si_2Ge_2$. Their arguments behind the presence of the entropy peak (and its absence in results for calorimetric measurements) differed considerably. Pecharsky and Gschneidner argue that (Pecharsky & Gschneidner, 1999):

> "The obvious sharp peak observed in $\Delta S_M(T)$ calculated from magnetization data significantly exceeds that calculated from heat capacity and is most likely associated with the fact that the magnetic transition occurs simultaneously with the crystal structure change in this alloy system. The magnetization data reflect only the changes in the magnetic entropy and are insensitive to the overlapping changes in the lattice entropy, while heat capacity data reflect the change in the combined entropies (lattice, electronic and magnetic), thus providing more reliable magnetocaloric effect values."

Giguère *et al.* in contrast argue that (Giguère et al., 1999):

> "The sudden, discontinuous entropy change is related to the phase transition itself, and is approximately independent of the applied field. The field shifts the transition only to higher temperatures. This entropy change cannot be calculated from the Maxwell relations, for two reasons: (i) It is not a magnetic entropy change, and (ii) M(T) or M(H) is not a continuous, derivable function. For first order transitions, the Clausius-Clapeyron (CC) equation offers a way to calculate the entropy change."

The arguments are in almost total disagreement with each other. The only point in common is that the direct use of the Maxwell relation on magnetization data would only report on the change of magnetic entropy, and not the change in 'non-magnetic' (lattice/electronic) entropy. Our analysis of this subject starts exactly in this point. What is 'magnetic entropy' and 'non-magnetic' entropy change, and why would non-magnetic entropy changes be invisible in magnetization measurements.

#### 4.1.1 Thermodynamics

Let us go back to some basics. To estimate entropy change from specific heat measurements, one needs to measure $C_p$ in both zero and non-zero applied field. The difference between curves, integrated in $T$, will then correspond to the entropy difference between the $H = 0$ and $H \neq 0$ conditions. This is rigorously the MCE, as seen by isothermal entropy change. On the other hand, magnetic measurements give us the bulk magnetization value, which is then used as a thermodynamic variable. If the dependence of $M$ on $H$ and $T$ is known, then the magnetic entropy change is easily calculated. The only possible entropy change that is invisible in magnetization measurements would then be the non-magnetically coupled entropy change in lattice/electronic degrees of freedom. Now, magnetization is defined thermodynamically as

$$M(H,T,p) = \left(\frac{\partial G}{\partial H}\right)_{T,p}, \tag{32}$$

so any change of the Gibbs free energy of system due to a change in applied field will then result on a change of the $M$ value. In other words, any change within the thermodynamic system that occurs due to a change in applied field has repercussions in $M$. And so the full magnetic entropy change is obtainable from $M(H,T)$. This point of view will become clearer upon investigating a magnetovolume coupling induced first-order phase transition. As we will show, the use of the CC relation does not allow us to calculate 'non-magnetic

entropy' variations, as the entropy change due to the lattice volume change is directly calculated from the use of the Maxwell relation. It is helpful to have a visual sense of the application of the Maxwell relation on magnetization data to obtain entropy change, as we will discuss in the following section. A summarized version of the following section is given in (Amaral & Amaral, 2010).

#### 4.1.2 Visual representation

Let us consider a second-order phase transition system. $M$ is a valid thermodynamic parameter, i.e., the system is in thermodynamic equilibrium and is homogeneous. Numerically integrating the Maxwell relation corresponds to integrating the magnetic isotherms in field, and dividing by the temperature difference:

$$\Delta S_M = \sum_0^{H'} \left( \frac{M_{i+1} - M_i}{T_{i+1} - T_i} \right) \Delta H_i = \frac{\int_0^{H'} [M(T_{i+1}, H) - M(T_i, H)]\, dH}{T_{i+1} - T_i} \tag{33}$$

which has a direct visual interpretation, as seen in Fig. 15(a).
If the transition is first-order, there is an 'ideal' discontinuity in the $M$ vs. $H$ plot. Still, apart from expected numerical difficulties, the area between isotherms can be estimated, (Fig. 15(b)).

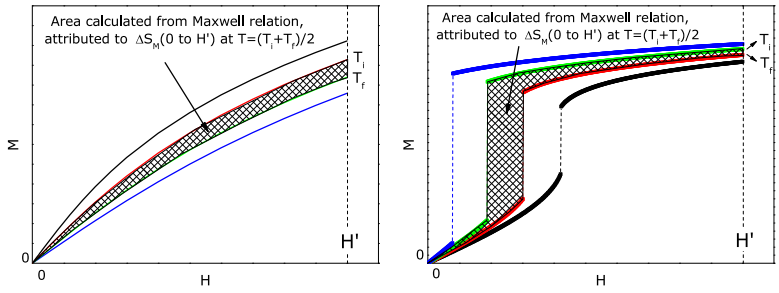


Fig. 15. Schematic diagrams of a a) second-order and b) first-order $M$ vs. $H$ plots, showing the area between magnetic isotherms. From Eq. 33 these areas directly relate to the entropy change.

The CC relation is presented in Eq. 34

$$\left| \frac{\Delta T}{\Delta H_C} \right| = \left| \frac{\Delta M}{\Delta S} \right|, \tag{34}$$

where $\Delta M$ is the difference between magnetization values before and after the discontinuity for a given $T$, $\Delta H_C$ is the shift of critical field from $\Delta T$ and $\Delta S$ is the difference between the entropies of the two phases.
The use of the CC relation to estimate the entropy change due to the first-order nature of the transition also has a very direct visual interpretation (Fig. 16(a)):
From comparing Figs. 15(b) and 16(a), we can see how all the magnetic entropy variation that can be accounted for with magnetization as the order parameter is included in calculations using the Maxwell relation (Fig. 16(b)).

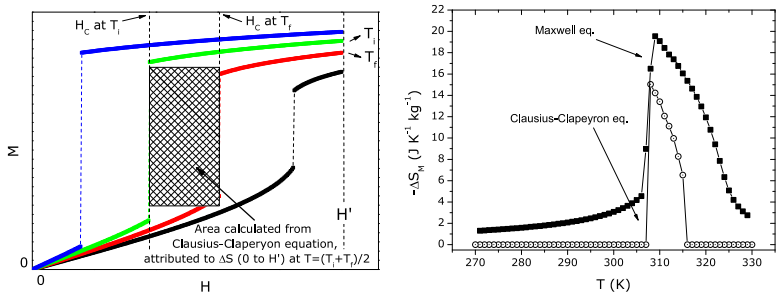


Fig. 16. a) schematic diagram of the area for entropy change estimation from the Clausius-Clapeyron equation, from a $M$ vs. $H$ plot of a magnetic first-order phase transition system, and b) magnetic entropy change versus temperature, estimated from the Maxwell relation (full symbols) and corresponding entropy change estimated from the Clausius-Clapeyron relation (open symbols).

All the magnetic entropy change is accounted for in calculations using the Maxwell relation. So there is no real gain nor deeper understanding of the systems to be had from the use of the CC relation to estimate magnetic entropy change. The 'non-magnetic entropy' is indeed accounted for by the Maxwell relation. The argument that the entropy peak exists, but specific heat measurements measure the lattice and electronic entropy in a way that conveniently smooths out this peak, is in contrast with the previously shown results. The entropy peak effect does not appear in calculations on purely simulated magnetovolume first-order transition systems, which seems to conflict with the arguments from Pecharsky and Gschneidner.

Of course, all of this reasoning and arguments have a common presumption: $M$ is a valid thermodynamic parameter. In truth, for a first-order transition, the system can present metastable states, and so the measured value of $M$ may not be a good thermodynamic parameter, and also the Maxwell relation is not valid. In the following section, the consequences of using non-equilibrium magnetization data on estimating the MCE is discussed.

### 4.2 Irreversibility effects

We consider simulated mean-field data of a first-order phase transition system, with the same initial parameters as used for the $M(H,T)$ data shown in Fig. 7(a), now considering the metastable and stable solutions of the transcendental equation. Results are shown in Fig. 17(a).

To assess the effects of considering the non-equilibrium solutions of $M(H,T)$ as thermodynamic variables in estimating the magnetic entropy change via the Maxwell relation, we use the three sets of $M(H,T)$ data. The result is presented in Fig. 17(b).

The use of the Maxwell relation on these non-equilibrium data produces visible deviations, and in the case of metastable solution (2), the obtained peak shape is quite similar to that reported by Pecharsky and Gschneidner for $Gd_5Si_2Ge_2$ (Pecharsky & Gschneidner, 1999). In this case $\Delta S_M(T)$ values from caloric measurements follow the half-bell shape of the equilibrium solution, but from magnetization measurements, an obvious sharp peak in $\Delta S_M(T)$ appears. Similar deviations have been interpreted as a result of numerical artifacts

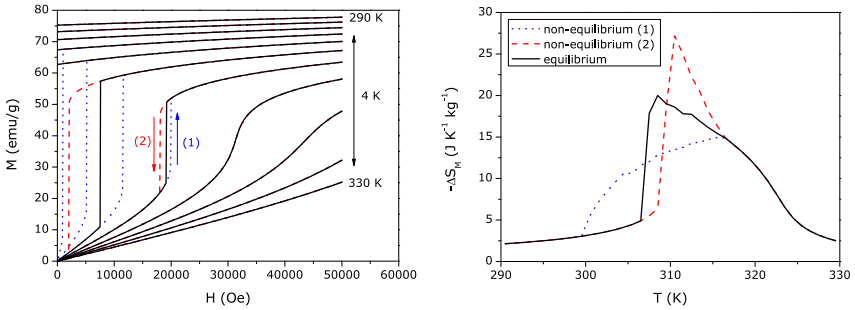


Fig. 17. a) $M$ versus $H$ isotherms from Landau theory, for a first-order transition, with equilibrium (solid lines) and non-equilibrium (dashed and dotted lines), and b) estimated $\Delta S_M$ versus $T$ for equilibrium and non-equilibrium solutions, from the use of the Maxwell relation.

(Wada & Tanabe, 2001), but are not present in a first-order system with no visible hysteresis (Hu et al., 2001).
For the considered model parameters, the overestimation of $\Delta S_M$ from using the Maxwell relation in nonequilibrium can be as high as $1/3$ of the value obtained under equilibrium, for an applied field change of 5 T.
For large values of $H$, where $M$ is near saturation in the paramagnetic region, the upper limit to magnetic entropy change, $\Delta S_M(\text{max}) = Nk_B\ln(2J+1)$, is reached, which for the chosen model parameters is $\sim 60$ J.K$^{-1}$.kg$^{-1}$. However, this is exceeded by around 10% by the use of the Maxwell relation to non-equilibrium values. If a stronger magneto-volume coupling is considered ($\lambda_3$ = 8 Oe (emu/g)$^{-3}$), the limit can be exceeded by $\sim 30$ J.K$^{-1}$kg$^{-1}$, clearly breaking the thermodynamic limit of the model, falsely producing a colossal MCE (Fig. 18).

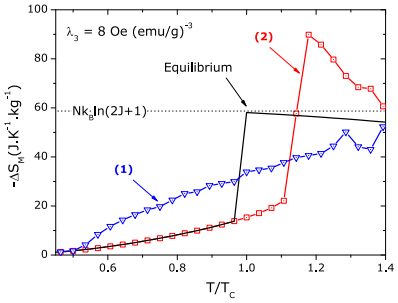


Fig. 18. $-\Delta S_M(T)$, obtained from the use of the Maxwell relation on equilibrium (black line) and metastable (colored lines) magnetization data from the Bean-Rodbell model with a magnetic field change of 1000 T.

The mean-field model also allows the study of mixed-state transitions, by considering a proportion of phases (high and low magnetization) within the metastability region. Magnetization curves are shown in the inset of Fig. 19, for $\lambda_3$ = 2 Oe (emu/g)$^{-3}$, corresponding to a critical field $\sim$ 10T. The mixed-phase temperature region is from 328 to

329 K, where the proportion of FM phase is set to 25% at 329 K, 50% at 328.5 K and 75% at 328 K.

The deviation resulting from using the mixed-state $M$ vs. $H$ curves and the Maxwell relation to estimate $\Delta S_M$ is now larger compared to the previous results (Fig. 19), since now the system is also inhomogeneous, further invalidating the use of the Maxwell relation. The thermodynamic limit to entropy change is again falsely broken. Note how the temperatures that exceed the limit of entropy change are the ones that include mixed-phase data to estimate $\Delta S_M$.

This result shows how the estimated value of $\Delta S_M$ can be greatly increased solely as a consequence of using the Maxwell relation on magnetization data from a mixed-state transition, which is the case of materials that show a colossal MCE (Liu et al., 2007). It is worth noting that, at this time, there are no calorimetric measurements that confirm the existence of the colossal MCE, and its report came from magnetization data and the use of the Maxwell relation.

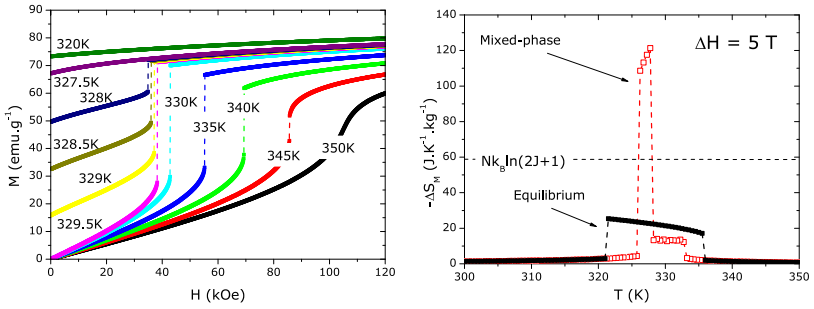


(a) (b)

Fig. 19. a) $M$ vs. $H$ isotherms of a mixed-phase system from the mean-field model and b) corresponding $\Delta S_M(T)$ for $\Delta H$=5T from Maxwell relation (open symbols), and of the equilibrium solution (solid symbols).

In the next section, an approach to make a realistic MCE estimation from mixed-phase magnetization data is presented.

### 4.3 Estimating the magnetocaloric effect from mixed-phase data

It is possible to describe a mixed-phase system, by defining a percentage of phases $x$, where one phase has an $M_1(H,T)$ magnetization value and the other will have an $M_2(H,T)$ magnetization value. In a coupled magnetostructural transition, one of the phases will be in the ferromagnetic state ($M_1$) and the other ($M_2$) will be paramagnetic. By changing the temperature, the phase mixture will change from being in a high magnetization state (ferromagnetic) to a low magnetization state (paramagnetic), and so the fraction of phases ($x$) will depend on temperature. Explicitly, this corresponds to considering the total magnetization of the system as $M_{\text{total}} = x(T)M_1 + (1-x(T))M_2$, for $H < H_c(T)$ and $M = M_1$ for $H > H_c(T)$, where $x$ is the ferromagnetic fraction in the system (taken as a function of temperature only), $M_1$ and $M_2$ are the magnetization of ferromagnetic and paramagnetic phases, respectively and $H_c$ is the critical field at which the phase transition completes.

So if we substitute the above formulation in the integration of the Maxwell relation, used to estimate magnetic entropy change, we can establish entropy change up to a field $H$ as

$$\Delta S_{\text{cal}} = \frac{d}{dT}\int_0^H [xM_1 + (1-x)M_2]\, dH' = \frac{\partial x}{\partial T}\int_0^H (M_1 - M_2) dH' + \Delta S_{\text{avg}} \tag{35}$$

for $H < H_c$, where

$$\Delta S_{\text{avg}} = x\int_0^H \frac{\partial M_1}{\partial T} dH' + (1-x)\int_0^H \frac{\partial M_2}{\partial T} dH'. \tag{36}$$

Out of these terms, $\Delta S_{\text{avg}}$ is due to the weighted contribution of the ferro- and paramagnetic phase in the system while the first term results from the phase transformation that occurred in the system during temperature and field variation. In order to obtain the entropy change up to a field above the critical magnetic field $H_c$, its temperature dependence plays an important role (latent heat contribution) and total entropy change can be formulated as

$$\begin{aligned}\Delta S_{\text{cal}} &= \frac{\partial}{\partial T}\int_0^{H_c(T)} [xM_1 + (1-x)M_2]\, dH' + \frac{\partial}{\partial T}\int_{H_c(T)}^H M_1 dH' \\ &= \frac{\partial x}{\partial T}\int_0^{H_c(T)} (M_1 - M_2) dH' + (1-x)\frac{\partial}{\partial T} H_c \left[M_1 - M_2\right]_{CT} + \Delta S_{\text{avg}} \\ &+ \int_{H_c(T)}^H \frac{\partial M_1}{\partial T} dH'. \end{aligned} \tag{37}$$

The first term in the previous expression represents the contribution of phase transformation, while the second term represents the fraction (1-$x$) of the latent heat contribution which is measured in the calorimetric experiment in the region of mixed state (since part of the sample is already in the ferromagnetic state, at zero field) and the last two terms are solely from the magnetic contribution.

For both $H < H_c$ and $H > H_c$ cases, the contribution from the temperature dependence of mixed phase fraction ($\partial x/\partial T$) represents the main effect from non-equilibrium in the thermodynamics of the system and therefore creates major source of error in the entropy calculation.

So, by estimating magnetic entropy change using the Maxwell relation and data from a mixed-phase magnetic system adds a non-physical term, which, as we will see later, can be estimated from analyzing the magnetization curves and the $x(T)$ distribution. Let us use mean-field generated data and a smooth sigmoidal $x(T)$ distribution (Fig. 20).

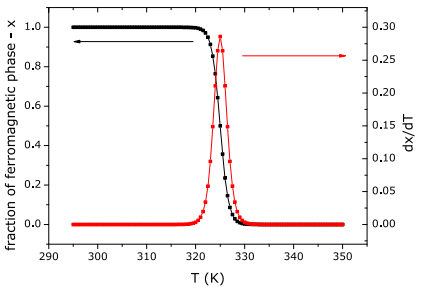


Fig. 20. Distribution of ferromagnetic phase of system, and its temperature derivative.

Such a wide distribution will then produce $M$ versus $H$ plots that strongly show the mixed-phase characteristics of the system, since the step-like behavior is well present (Fig.

21(a)). Using the Maxwell relation to estimate magnetic entropy change, we obtain the peak effect, exceeding the magnetic entropy change limit (Fig. 21(b)).

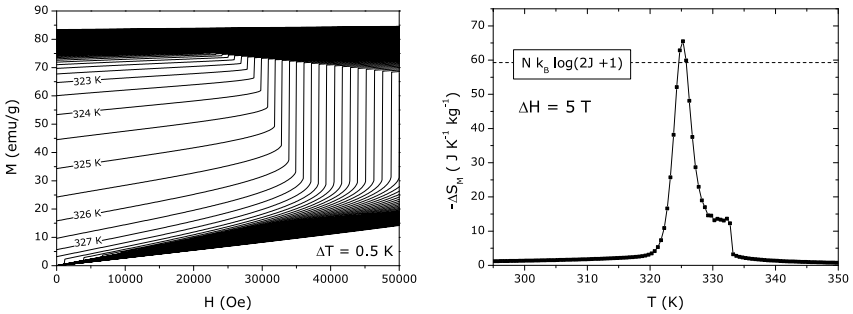


(a) (b)

Fig. 21. a) Isothermal $M$ versus $H$ plots of a simulated mixed-phase system, from 295 to 350 K (0.5 K step) and b) magnetic entropy change values resulting from the direct use of the Maxwell relation.

As the entropy plot shows us, the shape of the entropy curve and the $\partial x/\partial T$ function (Fig. 20) share a similar shape. This points us to Eqs. 35 or 37. It seems that the left side of the entropy plot may just be the result of the presence of the mixed-phase states, while for the right side of the entropy plot, there is some 'true' entropy change hidden along with the $\partial x/\partial T$ contribution. By using Eqs. 35 or 37, we present a way to separate the two contributions, and so estimate more trustworthy entropy change values. We plot the entropy change values obtained directly from the Maxwell relation, as a function of $\partial x/\partial T$. This is shown in Fig. 22(a), for the data shown in Figs. 21(a) and 20.

Plotting entropy change as a function of the temperature derivative of the phase distribution gives us a tool to remove the false $\partial x/\partial T$ contribution to the entropy change. As we can see in Fig. 22(a), there is a smooth dependence of entropy in $\partial x/\partial T$, which allows us to extrapolate the entropy results to a null $\partial x/\partial T$ value, following the approximately linear slope near the plot origin (dashed lines of Fig. 22(a)). This slope is constant as long and the magnetization difference between phases ($M_1 - M_2$) is approximately constant, which is observed in strongly first-order materials. The results of eliminating the $\partial x/\partial T$ contribution to the Maxwell relation result are presented in Fig. 22(b).

By eliminating the contribution of the temperature derivative of the mixed-phase fraction, the entropy 'peak' effect is eliminated, in a justified way. The resulting entropy curve resembles the results obtained from specific heat measurements when compared to results from magnetic measurements, as seen in Refs. (Liu et al., 2007) and (Tocado et al., 2009), among others.

However, this corrected entropy is always less than the value in equilibrium condition. This is because we deal with a fraction (1-$x$) of the phase $M_2$ remaining to transform which will give a fraction of latent heat entropy (Eq. 37) since part ($x$) of phase is already transformed at zero field. This average entropy change weighted by the fraction of each phase present, can be measured in calorimetric experiments. We regard $x(T)$ and $\partial x/\partial T$ as parameters that can be externally manipulated by changing the measurement condition/sample history and should therefore be carefully handled to obtain the true entropy calculation.

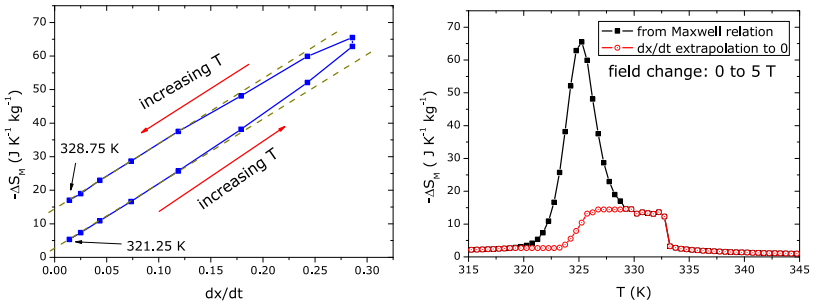


(a) (b)

Fig. 22. a) Entropy change, as obtained from the use of the Maxwell relation of mixed-phase magnetization data, versus a) $\partial x/\partial T$ and b) versus $T$, with values extrapolated to $\partial x/\partial T \rightarrow 0$.

We can conclude that, for a first-order magnetic phase transition system, estimating magnetic entropy change from the Maxwell relation can give us misleading results. If the system presents a mixed-phase state, the entropy 'peak' effect can be even more pronounced, clearly exceeding the theoretical limit of magnetic entropy change.

## 5. Acknowledgements

We acknowledge the financial support from FEDER-COMPETE and FCT through Projects PTDC/CTM-NAN/115125/2009, PTDC/FIS/105416/2008, CERN/FP/116320/2010, grants SFRH/BPD/39262/2007 (S. Das) and SFRH/BPD/63942/2009 (J. S. Amaral).

## 6. References

Aharoni, A. (2000). *Introduction to the Theory of Ferromagnetism*, Oxford Science Publications.

Amaral, J. S. & Amaral, V. S. (2009). The effect of magnetic irreversibility on estimating the magnetocaloric effect from magnetization measurements, *Appl. Phys. Lett.* 94: 042506.

Amaral, J. S. & Amaral, V. S. (2010). On estimating the magnetocaloric effect from magnetization measurements, *J. Magn. Magn. Mater.* 322: 1552.

Amaral, J. S., Reis, M. S., Amaral, V. S., Mendonça, T. M., Araújo, J. P., Sá, M. A., Tavares, P. B. & Vieira, J. M. (2005). Magnetocaloric effect in Er- and Eu-substituted ferromagnetic La-Sr manganites, *J. Magn. Magn. Mater.* 290: 686.

Amaral, J. S., Silva, N. J. O. & Amaral, V. S. (2007). A mean-field scaling method for first- and second-order phase transition ferromagnets and its application in magnetocaloric studies, *Appl. Phys. Lett.* 91(17): 172503.

Amaral, J. S., Tavares, P. B., Reis, M. S., Araújo, J. P., Mendonça, T. M., Amaral, V. S. & Vieira, J. M. (2008). The effect of chemical distribution on the magnetocaloric effect: A case study in second-order phase transition manganites, *J. Non-Cryst. Solids* 354: 5301.

Bean, C. P. & Rodbell, D. S. (1962). Magnetic disorder as a first-order phase transformation, *Phys. Rev.* 126(1): 104.

Brück, E. (2005). Developments in magnetocaloric refrigeration, *J. Phys D: Appl. Phys.* 38(23): R381.

Callen, H. B. (1985). *Thermodynamics and an introduction to thermostatistics*, 2nd edn, John Wiley and Sons, New York, USA.

Coey, J. (2009). *Magnetism and Magnetic Materials*, Cambridge University Press, Cambridge.

Das, S., Amaral, J. S. & Amaral, V. S. (2010a). Handling mixed-state magnetization data for magnetocaloric studies – a solution to achieve realistic entropy behaviour, *J. Phys D: Appl. Phys.* 43(15): 152002.

Das, S., Amaral, J. S. & Amaral, V. S. (2010b). Prediction of realistic entropy behavior from mixed state magnetization data for first order phase transition materials, *J. Appl. Phys.* 107(9): 09A912.

de Campos, A., Rocco, D. L., Carvalho, A. M. G., Caron, L., Coelho, A. A., Gama, S., da Silva, L. M., Gandra, F. C. G., dos Santos, A. O., Cardoso, L. P., Von Ranke, P. J. & de Oliveira, N. A. (2006). Ambient pressure colossal magnetocaloric effect tuned by composition in $Mn_{1-x}Fe_xAs$, *Nature Materials* 5(10): 802.

de Oliveira, N. A. & von Ranke, P. J. (2010). Theoretical aspects of the magnetocaloric effect, *Physics Reports-Review Section of Physics Letters* 489(4-5): 89.

Forsythe, G. E., Malcolm, M. A. & Moler, C. B. (1976). *Computer Methods for Mathematical Computations*, Prentice-Hall.

Gama, S., Coelho, A. A., de Campos, A., Carvalho, A. M. G., Gandra, F. C. G., von Ranke, P. J. & de Oliveira, N. A. (2004). Pressure-induced colossal magnetocaloric effect in MnAs, *Phys. Rev. Lett.* 93(23): 237202.

Giguère, A., Foldeaki, M., Gopal, B. R., Chahine, R., Bose, T. K., Frydman, A. & Barclay, J. A. (1999). Direct measurement of the "giant" adiabatic temperature change in $Gd_5Si_2Ge_2$, *Phys. Rev. Lett.* 83(11): 2262.

Gonzalo, J. A. (2006). *Effective Field Approach to Phase Transitions and Some Applications to Ferroelectrics*, World Scientific, Singapore.

Gschneidner Jr., K. A. & Pecharsky, V. K. (2008). Thirty years of near room temperature magnetic cooling: Where we are today and future prospects, *International Journal of Refrigeration* 31(6): 945.

Gschneidner Jr., K. A., Pecharsky, V. K. & Tsokol, A. O. (2005). Recent developments in magnetocaloric materials, *Reports on Progress in Physics* 68(6): 1479.

Gschneidner, K. A. & Pecharsky, V. K. (2000). Magnetocaloric materials, *Annual Review of Materials Science* 30: 387.

Hu, F. X., Shen, B. G., Sun, J. R., Cheng, Z. H., Rao, G. H. & Zhang, X. X. (2001). Influence of negative lattice expansion and metamagnetic transition on magnetic entropy change in the compound $LaFe_{11.4}Si_{1.6}$, *Appl. Phys. Lett.* 78(23): 3675.

Kittel, C. (1996). *Introduction to Solid State Physics*, 7th edn, John Wiley and Sons, New York.

Liu, G. J., Sun, J. R., Shen, J., Gao, B., Zhang, H. W., Hu, F. X. & Shen, B. G. (2007). Determination of the entropy changes in the compounds with a first-order magnetic transition, *Appl. Phys. Lett.* 90(3): 032507.

Pecharsky, V. K. & Gschneidner, K. A. (1997). Giant magnetocaloric effect in $Gd_5Si_2Ge_2$, *Phys. Rev. Lett.* 78(23): 4494.

Pecharsky, V. K. & Gschneidner, K. A. (1999). Heat capacity near first order phase transitions and the magnetocaloric effect: An analysis of the errors, and a case study of $Gd_5(Si_2Ge_2)$ and Dy, *J. Appl. Phys.* 86(11): 6315.

Phan, M. H. & Yu, S. C. (2007). Review of the magnetocaloric effect in manganite materials, *J. Magn. Magn. Mater.* 308(2): 325.

Rocco, D. L., de Campos, A., Carvalho, A. M. G., Caron, L., Coelho, A. A., Gama, S., Gandra, F. C. G., dos Santos, A. O., Cardoso, L. P., von Ranke, P. J. & de Oliveira, N. A. (2007). Ambient pressure colossal magnetocaloric effect in $Mn_{1-x}Cu_xAs$ compounds, *Appl. Phys. Lett.* 90(24): 242507.

Szewczyk, A., Szymczak, H., Wisniewski, A., Piotrowski, K., Kartaszynski, R., Dabrowski, B., Kolesnik, S. & Bukowski, Z. (2000). Magnetocaloric effect in $La_{1-x}Sr_xMnO_3$ for $x$ = 0.13 and 0.16, *Appl. Phys. Lett.* 77(7): 1026.

Tishin, A. M. & Spichin, Y. I. (2003). *The Magnetocaloric Effect and its Applications*, IOP Publishing, London.

Tocado, L., Palacios, E. & Burriel, R. (2009). Entropy determinations and magnetocaloric parameters in systems with first-order transitions: Study of MnAs, *J. Appl. Phys.* 105: 093918.

Wada, H. & Tanabe, Y. (2001). Giant magnetocaloric effect of $MnAs_{1-x}Sb_x$, *Appl. Phys. Lett.* 79(20): 3302.

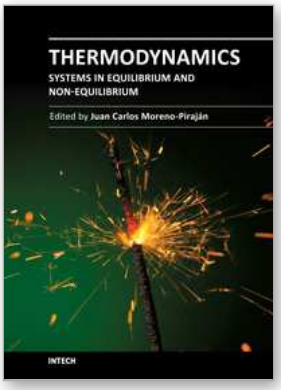


**Thermodynamics - Systems in Equilibrium and Non-Equilibrium**
Edited by Dr. Juan Carlos Moreno PirajÃ¡n

ISBN 978-953-307-283-8
Hard cover, 306 pages
**Publisher** InTech
**Published online** 10, October, 2011
**Published in print edition** October, 2011

Thermodynamics is one of the most exciting branches of physical chemistry which has greatly contributed to the modern science. Being concentrated on a wide range of applications of thermodynamics, this book gathers a series of contributions by the finest scientists in the world, gathered in an orderly manner. It can be used in post-graduate courses for students and as a reference book, as it is written in a language pleasing to the reader. It can also serve as a reference material for researchers to whom the thermodynamics is one of the area of interest.

**How to reference**
In order to correctly reference this scholarly work, feel free to copy and paste the following:

J. S. Amaral, S. Das and V. S. Amaral (2011). The Mean-Field Theory in the Study of Ferromagnets and the Magnetocaloric Effect, Thermodynamics - Systems in Equilibrium and Non-Equilibrium, Dr. Juan Carlos Moreno PirajÃ¡n (Ed.), ISBN: 978-953-307-283-8, InTech, Available from: http://www.intechopen.com/books/thermodynamics-systems-in-equilibrium-and-non-equilibrium/the-mean-field-theory-in-the-study-of-ferromagnets-and-the-magnetocaloric-effect

INTECH
open science | open minds

**InTech Europe**
University Campus STeP Ri
Slavka Krautzeka 83/A
51000 Rijeka, Croatia
Phone: +385 (51) 770 447
Fax: +385 (51) 686 166
www.intechopen.com

**InTech China**
Unit 405, Office Block, Hotel Equatorial Shanghai
No.65, Yan An Road (West), Shanghai, 200040, China
中国上海市延安西路65号上海国际贵都大饭店办公楼405单元
Phone: +86-21-62489820
Fax: +86-21-62489821